European Journal of Pharmaceutical Sciences 214 (2025) 107280

Contents lists available at ScienceDirect

European Journal of Pharmaceutical Sciences

journal homepage: www.elsevier.com/locate/ejps

Predicting Caco-2/MDCK intrinsic membrane permeability from HDM-PAMPA-derived hexadecane/water partition coefficients

Carolin Dahley [a], Kai-Uwe Goss [a,b], Andrea Ebert [a,*]

[a] Department of Computational Biology & Chemistry, Helmholtz Centre for Environmental Research (UFZ), Permoserstraße 15, 04318 Leipzig, Germany
[b] Institute of Chemistry, University of Halle-Wittenberg, Kurt-Mothes-Straße 2, 06120 Halle, Germany

ARTICLE INFO

Key words:
HDM-PAMPA
hexadecane/water partition coefficient
Caco-2
MDCK
intrinsic membrane permeability
solubility-diffusion model

ABSTRACT

Reliable membrane permeability data are essential in early drug development. Therefore, there is a strong need for robust experimental high-throughput screening methods, or ideally, accurate predictive tools, to assess membrane permeability. In a previous study, we demonstrated that the solubility-diffusion model can successfully predict passive permeability across biological Caco-2 and MDCK membranes, provided accurate hexadecane/water partition coefficients ($K_{hex/w}$) are available.

In this study, we investigated the HDM-PAMPA method for determining $K_{hex/w}$. We measured our own data (64 compounds) using this assay and compared the results with established methods such as black lipid membrane (BLM) experiments and classical two-phase systems. Our results show good agreement across methods, with both our data and literature values aligning closely.

Using these experimentally determined $K_{hex/w}$ values, we achieved accurate predictions of permeability in Caco-2 and MDCK cell membranes (RMSE = 0.8, n = 29) based on a previously calibrated equation. We further evaluated the *in silico* prediction of $K_{hex/w}$ using the UFZ-LSER database and the software COSMOtherm. COSMOtherm performed nearly as well as experimental measurements (RMSE = 1.20, n = 29), while the LSER approach (RMSE = 1.63, n = 29) is best applied when experimental descriptors are available or as a complement to COSMOtherm. This work highlights the practical utility of $K_{hex/w}$ in high-throughput permeability estimation, which can support efficient screening and prioritization of drug candidates in pharmaceutical research.

1. Introduction

Intrinsic membrane permeability (P_0), defined as the pH-independent passive membrane permeability of the neutral species, is a key parameter in drug development, as it critically affects a compound's absorption, distribution, metabolism and excretion (Di et al., 2020; Fagerholm, 2008). The *in vitro* gold standard for predicting permeability, particularly in the gastrointestinal tract, are cell-based assays (Hubatsch et al., 2007). These assays measure the transport of a compound from the donor to the acceptor compartment across a Caco-2 (human colorectal adenocarcinoma) or MDCK (Madin-Darby canine kidney) cell monolayer grown on a permeable filter support. However, they are associated with several limitations, including high time and cost demands and a considerable risk of erroneous data evaluation (Ebert et al., 2024). Consequently, a reliable *in silico* approach for predicting $P_{0,Caco\text{-}2/MDCK}$ is highly desirable.

In our recent work (Dahley et al., 2024), we demonstrated that $P_{0,Caco\text{-}2/MDCK}$ is reliably predicted by the solubility-diffusion model-derived intrinsic membrane permeability ($P_{0,SDM}$) using the following empirical correlation:

$$\log P_{0,Caco-2/MDCK} = 0.84 \cdot \log P_{0,SDM} - 1.85 \quad (1)$$

Assuming that the hydrophobic membrane interior represents the main barrier to permeation (Bittermann and Goss, 2017; Lomize and Pogozheva, 2019) and is well-modelled by hexadecane (Finkelstein, 1976; Walter and Gutknecht, 1986), $P_{0,SDM}$ is calculated from the diffusion coefficient of the compound in hexadecane (D_{hex}), its partition coefficient between hexadecane and water ($K_{hex/w}$) and the thickness of the hexadecane-like membrane interior (x_m):

$$P_{0,SDM} = \frac{D_{hex} \cdot K_{hex/w}}{x_m} \quad (2)$$

While both D_{hex} and x_m can be estimated with reasonable accuracy, the key parameter for reliably predicting $P_{0,Caco\text{-}2/MDCK}$ is $K_{hex/w}$. In our

* Corresponding author.
E-mail address: andrea.ebert@ufz.de (A. Ebert).

https://doi.org/10.1016/j.ejps.2025.107280
Received 23 July 2025; Received in revised form 9 September 2025; Accepted 16 September 2025
Available online 17 September 2025

previous work (Dahley et al., 2024), $K_{hex/w}$ was successfully predicted from experimental linear solvation energy relationship (LSER) descriptors using the UFZ-LSER database. However, experimental LSER descriptors are available only for a limited number of compounds and their determination is time-consuming. Using predicted instead of experimental descriptors increases the uncertainty in $K_{hex/w}$. It therefore remains to be determined whether $K_{hex/w}$ can be reliably predicted using an alternative tool such as COSMOtherm or accurately measured using a high-throughput method.

The partition coefficient of a compound is typically measured in a system of two immiscible phases (e.g. stir-flask method, shake-flask method). It is defined as the ratio of concentrations in both phases at equilibrium (Berthelot and Jungfleisch, 1872). However, extracting $K_{hex/w}$ from two-phase systems is time-consuming and complex since it can be affected by temperature, time to equilibration, measurement in one or both phases, solute concentration, degradation, purity of materials, buffer, centrifugation and phase volume ratio (see Dearden and Bresnen (1988) for details). A reliable high-throughput alternative to the standard two-phase system for determining $K_{hex/w}$ would therefore be highly advantageous.

Besides the conventional two-phase system, $K_{hex/w}$ can also be derived from permeability assays, using the rearranged form of Eq. (2). One such example is the black lipid membrane (BLM) assay, which demonstrates a strong correlation between membrane permeability and $K_{hex/w}$ (Walter and Gutknecht, 1986). Unfortunately, BLM assays are not suitable for high-throughput screening. A widely used high-throughput method for determining permeability in pharmaceutical research is the Parallel Artificial Membrane Permeability Assay (PAMPA). Similar to Caco-2/MDCK assays, PAMPA assays consist of two compartments, donor and acceptor, separated by a filter. However, unlike the Caco-2/MDCK assays, no cells are seeded onto the filter; instead, it is impregnated with lipid (e.g. egg lecithin, DOPC, phospholipid mixtures). This approach is questionable, as the lipid in PAMPA does not form a well-defined bilayer structure like that found in artificial black lipid membranes or biological membranes (Assmus et al., 2017). To address this limitation, Wohnsland and Faller (2001) introduced HDM-PAMPA, which uses hexadecane instead of lipid. Based on a dataset of 16 compounds they demonstrated strong agreement between the $K_{hex/w}$ obtained from a two-phase system and those derived from HDM-PAMPA. Consequently, HDM-PAMPA could serve as a promising high-throughput method for determining $K_{hex/w}$, which could subsequently be used to predict $P_{0,Caco\text{-}2/MDCK}$ according to Eqs. (1) and (2).

Given this potential, we conducted new HDM-PAMPA measurements to evaluate their utility in predicting $P_{0,Caco\text{-}2/MDCK}$. The specific objectives of this work were to: (i) validate HDM-PAMPA as a reliable method for determining log $K_{hex/w}$ by comparing the log $K_{hex/w}$ extracted from our own HDM-PAMPA permeability assays to those extracted from two-phase systems, BLM permeability assays and to literature-reported HDM-PAMPA permeability data, (ii) assess the reliability of log $K_{hex/w}$ predictions by comparing the log $K_{hex/w}$ extracted from our own and literature HDM-PAMPA permeability assays to those predicted by the UFZ-LSER database and COSMOtherm, (iii) demonstrate the accuracy of predicting $P_{0,Caco\text{-}2/MDCK}$ from HDM-PAMPA-derived log $K_{hex/w}$ according to Eqs. (1) and (2) by comparing experimental and predicted $P_{0,Caco\text{-}2/MDCK}$ and (iv) determine whether LSER- or COSMOtherm-predicted log $K_{hex/w}$ can serve as a viable alternative to HDM-PAMPA-derived log $K_{hex/w}$ for predicting $P_{0,Caco\text{-}2/MDCK}$ by comparing experimental and predicted $P_{0,Caco\text{-}2/MDCK}$.

2. Material and methods

2.1. Selection of compounds

To assess whether the experimental log $K_{hex/w}$ obtained from HDM-PAMPA allow for accurate prediction of $P_{0,Caco\text{-}2/MDCK}$ according to Eq. (1), we selected only compounds for which high-quality experimental $P_{0,Caco\text{-}2/MDCK}$ are available. Specifically, we focused on the 39 compounds whose experimental $P_{0,Caco\text{-}2/MDCK}$ were classified as highly reliable (category 1a) by Ebert et al. (2024). Ten of these compounds were excluded because either their acquisition (bremazocine, ephedrine, meprobamate, morphine) or measurement (cimetidine, creatinine, cyclosporin A, triamterene, urea, vinblastine) was not feasible. Additionally, 26 and 12 compounds were selected for their relevance to an upcoming paper on blood-brain barrier permeability and active transport, respectively. All chemicals and their respective suppliers are listed in Table S1–1 in the Supplementary Material 1.

2.2. Prediction methods

2.2.1. COSMOtherm

The COSMOtherm (2018) approach (Eckert and Klamt, 2002; Klamt, 1995; Klamt et al., 1998) is based on the Conductor-like Screening Model for Realistic Solvation (COSMO-RS) theory. Starting from the molecular structure of a solute or solvent, quantum chemical calculations are used to determine the polarization charge density on the molecular surface in the presence of an embedding conductor (COSMOfiles). Pairwise interaction energies between these surfaces are then calculated and thermodynamically averaged over many ensembles. This procedure allows the prediction of physicochemical properties such as partition coefficients at infinite dilution. See Eckert and Klamt (2002) for details. The BP-TZVPD-FINE level of theory was employed for all COSMO-RS calculations.

2.2.2. LSER

The linear solvation energy relationship (LSER) approach (Endo and Goss, 2014) provides a framework to predict solute partitioning between two phases based on molecular interactions. For hexadecane-water systems, the partition coefficient $K_{hex/w}$ at 25 °C is expressed as:

$$log\ K_{hexw} = 0.67E - 1.62S - 3.59A - 4.87B + 4.43V + 0.09 \quad (3)$$

Here, the solute descriptors represent key physicochemical properties: E includes the excess molar refraction, S accounts for polarity and polarizability, A and B describe hydrogen-bond acidity and basicity, and V is the McGowan characteristic volume. Each term reflects the interaction of the solute with the surrounding phase, capturing contributions from van der Waals forces, hydrogen bonding, and cavity formation.

Experimental solute descriptors were either taken from the UFZ-LSER database (2025) if available, or predicted by UFZ-LSER database, the Beta EAS-E Suite (2025), or with ACD/Percepta (2020).

2.3. HDM-PAMPA assay

2.3.1. Transport experiments

The HDM-PAMPA transport experiments were conducted using the iso-pH method, where the donor and acceptor pH are identical, to avoid complications in evaluating the experiments (Dahley et al., 2023). The pH was carefully selected to ensure that the hexadecane layer, rather than the omnipresent aqueous boundary layer (ABL), served as the primary permeation barrier. The following buffers were used for pH adjustment: 10 mM β-alanine (pH 4), 5 mM β-alanine and 5 mM MES (pH 5), 10 mM MES (pH 6), 10 mM MOPS (pH 7), 10 mM TAPS (pH 8–9) and 10 mM CAPSO (pH 10). Stock solutions of the test compounds (1–5000 μg/ml) were prepared directly in buffer when possible. Sparingly soluble compounds were initially dissolved in DMSO and then diluted with buffer. The DMSO content was kept identical in both the buffer and stock solution, never exceeding 1 %. Each stock solution was filtered through a glass fibre syringe filter (pore size: 0.7 μm, diameter: 13 mm, Carl Roth GmbH+Co. KG, Karlsruhe, Germany) before use to remove undissolved particles.

The HDM-PAMPA setup consisted of a bottom MultiScreen Transport Receiver Plate (Cat. No.: MATRNPS50, Merck KGaA, Darmstadt, Germany) and a top MultiScreen IP Filter Plate (pore size: 0.45 μm, filter

thickness: 100–145 μm, filter area: 0.3 cm^2, Cat. No.: MAIPN4550, Merck KGaA, Darmstadt, Germany). The filters were impregnated with 3.5 μl of hexadecane. Using smaller amounts of hexadecane led to uneven filter wetting, while larger amounts caused excess hexadecane to accumulate on the donor compartment surface, forming grease-like spots. While 280 μl of buffer were added to the bottom acceptor compartment, 200 μl of stock solution were added to the top donor compartment. Using smaller buffer volumes in the acceptor compartment led to the formation of air bubbles between the acceptor buffer and the filter, reducing the available permeation area. The assembled PAMPA plates were incubated at 37 °C in a TH30 incubator (Edmund Bühler GmbH, Bodelshausen, Germany). To minimize evaporation, the PAMPA plates were placed in a desiccator filled with water instead of desiccant to maintain a consistently high humidity, thereby reducing evaporation to below 10 %.

Samples from both compartments were collected after 4, 24 or 96 h, depending on the expected permeability. Preliminary tests indicated that some compounds strongly adsorb to the surface of the PAMPA plates, leading to a significant underestimation of permeability. To saturate adsorption, the stock solution concentrations were maximized. Additionally, the acceptor plate was extracted with 280 μl of ethanol at room temperature after the transport experiment. To enhance extraction efficiency, the compound was kept as neutral as possible during the extraction. Depending on the compound's pK_a, either pure EtOH or EtOH supplemented with 1 % CAPSO (pH 10) or 1 % β-Ala (pH 4) was used. Extraction of the donor plate was not feasible, as ethanol caused cracks in the donor plate. Samples from the acceptor compartment were collected after 1 h. Sample concentrations were analyzed using an Infinity II 1260 LC system coupled to a 6420 triple quadrupole with ESI source (Agilent Technologies Inc., Santa Clara, USA). Transport experiments for each compound were conducted at least in three technical replicates. Pre-tests assessing inter-day reproducibility, as well as experiments conducted at different pH values (where the hexadecane barrier was the dominant resistance), and varying experimental durations yielded comparable hexadecane/water partition coefficients (data not shown).

2.3.2. Extraction of $K_{hex/w}$

From the concentrations determined in HDM-PAMPA assays, apparent permeability (P_{app}), corrected for recovery and non-sink conditions, was calculated according to Eqs. S1–1a and 1b.

P_0 could only be derived from P_{app} if P_{ABL} contributed <50 % to the total transport resistance. In these cases, P_0 was derived from P_{app} using the following equation:

$$P_0 = \frac{1}{\frac{1}{P_{app}} - \frac{1}{P_{ABL}}} \cdot \frac{1}{f_n} \quad (4)$$

Where P_{ABL} is the ABL permeability and f_n is the neutral fraction of the compound at the experimental pH. P_{ABL} was calculated by dividing the diffusion coefficient of the compound in water (estimated from the molecular weight according to Eq. S1–2b) by the thickness of the ABL. The thickness of the ABL was experimentally determined to be 1112 ± 65 μm, based on the permeability of the lipophilic acid diclofenac at pH 4. The calculation of f_n and the required pK_a values are provided in Eqs. S1–3a to 3d and Table S1–2.

Based on P_0, $K_{hex/w}$ was calculated according to the solubility-diffusion model:

$$K_{hex/w} = \frac{P_0 \cdot x_{filter}}{D_{hex,37°C} \cdot \varepsilon_{filter}} \quad (5)$$

Where x_{filter} is the average filter thickness (125 μm) and ε_{filter} is the porosity of the filter (0.7). In the literature, apparent porosity as described in Nielsen and Avdeef (2004) is sometimes used in permeability evaluations. This approach assumes the presence of excess lipid layers on both sides of the filter, effectively increasing the "apparent" porosity of the lipid layer and its thickness. We refrained from using apparent porosity, because i) this did not increase the extracted $K_{hex/w}$ by more than a factor of 1.2, and ii) because we observed the accumulation of the surplus hexadecane at the donor compartments surface, indicating that it could not fully form a thicker membrane layer as assumed in the calculation of apparent porosity. D_{hex} is the diffusion coefficient of the compound in hexadecane (estimated from the molecular weight according to Eq. S1–2d).

2.4. BLM assay

2.4.1. Transport experiments

Analogous to the HDM-PAMPA transport experiments, BLM transport experiments were conducted using the iso-pH method with the same buffer systems. Stock solutions of the three test compounds clonidine, sumatriptan and theophylline (300–1500 μg/mL) were prepared directly in the respective buffer. Transport of the test compound across a black lipid membrane composed of DPhPC with physiological amounts of cholesterol and sphingomyelin was assessed at room temperature. Membrane integrity was confirmed by capacitance measurements. Samples from the acceptor compartment were collected every 30 min and analyzed by LC-MS/MS. For detailed methodology, see Dahley et al. (2022; 2024).

2.4.2. Extraction of log $K_{hex/w}$

The P_{app} for amantadine, diclofenac, luvastatin, metoprolol, salicylic acid and venlafaxine were determined in Dahley et al. (2022). The P_{app} for acebutolol, chloroquine, pindolol, ranitidine, rizatriptan, scopolamine and talinolol were reported in Dahley et al. (2024). The P_{app} for clonidine, sumatriptan and theophylline were determined analogously in this work.

Analogous to HDM-PAMPA assays, P_0 can be calculated from P_{app} using Eq. (4).

Assuming that the hexadecane-like membrane interior serves as the primary permeation barrier, $K_{hex/w}$ in BLM assays can be extracted from P_0 in a similar manner as $K_{hex/w}$ in HDM-PAMPA assays:

$$K_{hex/w} = \frac{P_0 \cdot x_m}{D_{hex,25°C}} \quad (6)$$

Where x_m is the thickness of the hexadecane-like membrane interior (40 Å) and D_{hex} is the diffusion coefficient of the compound in hexadecane (estimated from the molecular weight according to Eq. S1–2c). A factor ε, as in Eq. (5), is not required since black lipid membranes are free-standing membranes without filter support.

2.5. Extraction of log $K_{hex/w}$ from literature HDM-PAMPA P_{app}

$K_{hex/w}$ values were derived from literature-reported HDM-PAMPA permeability data (Bujard et al., 2014; 2017; Nagahara et al., 2004; Petit et al., 2016; Rolando et al., 2010; Von Richter et al., 2009; Wohnsland and Faller, 2001). The stated P_{app} already included porosity effects, which is inappropriate in this context, as porosity does not influence transport across the ABL. Therefore, we corrected the reported P_{app} by multiplying with the porosity factor used in the respective studies.

We defined lower cut-off thresholds for permeability values, analogous to those used for paracellular transport in Caco-2 and MDCK cell assays, to account for potential artifacts such as water channel leakage (Avdeef, 2012; Tsinman et al., 2011) or the sensitivity limits of UV detection. P_{app} values that did not exceed this threshold were excluded from P_0 determination. Similarly, measurements within a factor of two below the expected permeability of the ABL were also considered unreliable for P_0 extraction. Extracted ABL sizes and used lower cut-off values are stated in Table S1–3.

Additionally, if the log partition coefficient between water and hexadecane at the experimental pH (log $D_{hex/w}$) exceeded 3, the data

were excluded due to possible retention effects. These effects are not adequately addressed by the standard correction method, as the hexadecane layer is unlikely to be in equilibrium with the donor compartment under such conditions (Ebert et al., 2024). Only four datapoints were affected by this retention criterion. For two of these, amitriptyline and chlorpromazine, literature data show that measurements at different pH values resulted in substantially higher log $K_{hex/w}$ values (see Table S2–2 for details).

Although these strict exclusion criteria may have also removed some data from which P_0 values could potentially have been extracted, they are necessary to ensure a high-quality dataset.

$K_{hex/w}$ was subsequently calculated from P_0 using Eq. (5). The pK_a values used for the extraction and the resulting $K_{hex/w}$ values are provided in Tables S2–1 and S2–2.

3. Results and discussion

3.1. Comparison of $K_{hex/w}$ from HDM-PAMPA and alternative methods

3.1.1. $K_{hex/w}$ from two-phase systems

Following the findings of Wohnsland and Faller (2001) regarding the suitability of HDM-PAMPA for determining $K_{hex/w}$, we compared log $K_{hex/w}$ obtained from our own HDM-PAMPA experiments with literature data obtained from two-phase systems (see Fig. 1A).

Overall, there was good agreement between the $K_{hex/w}$ determined with both methods. Deviations were within approximately one order of magnitude, which is consistent with the known variability in partition coefficient measurements using two-phase systems. As shown in Table S1–4, log $K_{hex/w}$ - and other partition coefficients such as the octanol/water partition coefficient (log $K_{o/w}$) (Bahadur et al., 1997; Dearden and Bresnen, 1988) - can vary by up to two log units for the same compound, depending on the reference.

Minor deviations may also be attributed to differences in measurement temperature. While the $K_{hex/w}$ in this work and in Yazdanian et al. (1998) were determined at 37 °C, those of Walter and Gutknecht (1984) and Wohnsland and Faller (2001) were determined at room temperature. However, based on data from other partition coefficients such as $K_{o/w}$, this temperature difference is unlikely to significantly impact $K_{hex/w}$ (Bahadur et al., 1997).

One compound, however, stands out with a deviation of almost three orders of magnitude: acebutolol. This discrepancy may originate from the experimental setup used by Yazdanian et al. (1998). Assuming a log $K_{hex/w}$ of −3.20 for acebutolol, as determined in our HDM-PAMPA experiments, the resulting log $D_{hex/w}$ at pH 7.4 would be −4.99. Given the equal volumes of hexadecane and water used in Yazdanian's setup, this would imply that 99.999 % of the compound resided in the aqueous phase, with only 0.001 % in the hexadecane phase. It is likely that the analytical sensitivity of their method was insufficient to accurately quantify such low concentrations. In fact, this highlights a key limitation of the two-phase method: its reliability decreases significantly when the amount of compound is extremely small in one phase and extremely high in the other phase, restricting the method's application range.

3.1.2. $K_{hex/w}$ from BLM assays

Due to the limitations of the two-phase system, we subsequently compared the log $K_{hex/w}$ obtained from our own HDM-PAMPA permeability assays with those derived from an alternative permeability assay, the BLM assay (see Fig. 1B).

Similar to Fig. 1A, a high level of agreement was observed between log $K_{hex/w}$ from HDM-PAMPA and BLM. Minor deviations may again be attributed to temperature differences during measurement, as HDM-PAMPA experiments were conducted at 37 °C, while the BLM experiments were performed at room temperature. The BLM setup is highly sensitive to vibrations and was therefore not placed inside an incubator.

In contrast to Fig. 1A, where the two-phase system produced an outlying value for acebutolol, log $K_{hex/w}$ determined by HDM-PAMPA and BLM shows excellent agreement. This confirms that the two-phase method may be unreliable for compounds with very low distribution into the hexadecane phase. More importantly, it demonstrates that permeability-based methods like HDM-PAMPA and BLM can accurately measure log $K_{hex/w}$ over a broader range of values, including compounds with very low hexadecane affinity, extending the applicability of partition coefficient determination beyond the limits of the conventional two-phase approach.

3.1.3. $K_{hex/w}$ from HDM-PAMPA from literature

As discussed in Section 3.1.1, the partition coefficients determined in the conventional two-phase system exhibit high variability. To assess the comparability of log $K_{hex/w}$ obtained from HDM-PAMPA across different laboratories and experimental setups, we compared log $K_{hex/w}$ from our own HDM-PAMPA experiments with those extracted from HDM-PAMPA data in the literature (see Fig. 1C).

The main difference between the experimental setups is the thickness of the filter - and consequently, the thickness of the hexadecane layer. Filters used in this work had an average thickness of 125 µm, while those used by Wohnsland and Faller (2001), Von Richter et al. (2009) and Bujard et al. (2017) were considerably thinner at approximately 10 µm. The detection method also varied, with mass spectrometry used in this work and UV absorption used in the other studies. Additionally, experiments in this work were conducted at 37 °C, while the literature data

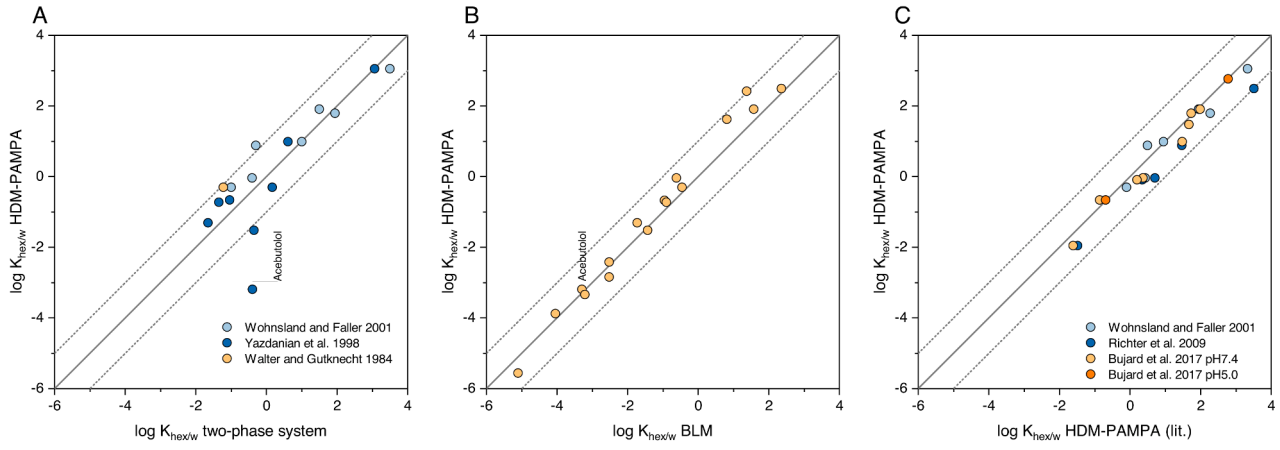

Fig. 1. Comparison of log $K_{hex/w}$ derived from HDM-PAMPA assays (see Table S1–5) with A) log $K_{hex/w}$ derived from two-phase systems, B) log $K_{hex/w}$ derived from BLM assays (see Table S1–6) and C) log $K_{hex/w}$ derived from HDM-PAMPA assays in the literature (see Table S2–1). The gray solid line represents the line of identity, deviations of ±1 log unit are shown as gray dotted lines.

were obtained at room temperature.

As shown in Fig. 1C, there is good agreement between the log $K_{hex/w}$ determined in this work and those extracted from literature data. Similar to Fig. 1A and 1B, deviations rarely exceed one order of magnitude. This suggests that the determined log $K_{hex/w}$ are well reproducible, regardless of filter thickness, detection method or temperature. The application range, however, is influenced by filter thickness and detection method. The use of thicker filters increases the relative contribution of the hexadecane layer to the overall resistance, enabling the measurement of compounds that are ABL-limited in setups with thinner filters and thus expanding the application range toward higher log $K_{hex/w}$. The use of LC-MS/MS instead of UV detection improves analytical sensitivity, enabling the quantification of lower concentrations and thus expanding the application range toward lower log $K_{hex/w}$.

Overall, HDM-PAMPA appears to be a reliable and robust method for determining $K_{hex/w}$, offering less variance and a broader application range than conventional two-phase systems.

3.2. Comparison of experimental $K_{hex/w}$ from HDM-PAMPA and predicted $K_{hex/w}$

3.2.1. Prediction of $K_{hex/w}$ using the UFZ-LSER database

Although HDM-PAMPA enables high-throughput determination of experimental $K_{hex/w}$, a reliable method for predicting $K_{hex/w}$ would be highly desirable.

One such approach is based on Linear Solvation Energy Relationship (LSER) descriptors, as provided by the UFZ-LSER database (2025). This database offers experimental descriptors for a large number of compounds and additionally allows the calculation of LSER descriptors directly from a compound's Simplified Molecular Input Line Entry System (SMILES) code. We compared the $K_{hex/w}$ obtained from our own HDM-PAMPA experiments with those predicted from LSER descriptors using the UFZ-LSER database (see Fig. 2A). The LSER descriptors were prioritized according to their expected reliability: experimental descriptors (UFZ-preselected published values) > experimental descriptors (Abraham Absolv, not preselected) > calculated descriptors.

When considering only log $K_{hex/w}$ predicted using experimental LSER descriptors from the UFZ-preselected published dataset, there is good agreement with the experimental log $K_{hex/w}$ from HDM-PAMPA ($n = 19$, RMSE = 0.77), with deviations rarely exceeding one order of magnitude.

A lower degree of agreement between experimental and predicted log $K_{hex/w}$ is observed when experimental descriptors from the Abraham Absolv dataset are used ($n = 28$, RMSE = 1.64). Although these are experimental descriptors, the prediction accuracy varied substantially – while some predicted log $K_{hex/w}$ closely matched the experimental log $K_{hex/w}$ from HDM-PAMPA, others deviated by more than three orders of magnitude. This variability arises from the differing reliability of the experimental descriptors, which is strongly influenced by the quality, quantity and diversity of the experimental partition coefficients used for their calibration (Endo and Goss, 2014).

As expected, the poorest agreement was observed when using calculated UFZ-LSER descriptors ($n = 17$, RMSE = 2.13), with deviations reaching nearly five orders of magnitude. To evaluate whether alternative tools for calculating LSER descriptors provide better agreement, we compared the $K_{hex/w}$ predicted from calculated LSER descriptors from UFZ-LSER database with ACD/Percepta ($n = 17$, RMSE = 1.59) and Beta EAS-E Suite (2025) ($n = 17$, RMSE = 2.46), see Table S1–7. However, even with these alternative tools, deviations of more than three orders of magnitude between predicted and experimental log $K_{hex/w}$ were still observed.

In summary, predicting log $K_{hex/w}$ based on UFZ-preselected LSER descriptors is quite accurate. However, for compounds lacking UFZ-preselected LSER descriptors—such as newly developed compounds—using the UFZ-LSER database is not reliable, as the uncertainty in log $K_{hex/w}$ predicted from Abraham Absolv or calculated LSER descriptors can be extremely high.

3.2.2. Prediction of $K_{hex/w}$ using COSMOtherm

Given the insufficient reliability of the UFZ-LSER database in predicting $K_{hex/w}$, we subsequently compared the log $K_{hex/w}$ from our own HDM-PAMPA experiments with those predicted by the commercial COSMOtherm software (see Fig. 2B).

As shown in Fig. 2B, there is good agreement between experimental and predicted log $K_{hex/w}$ ($n = 64$, RMSE =1.02). However, sulfadiazine stands out as an outlier with a deviation of >2.5 log units, which might be attributed to its tautomers. In our COSMOtherm calculations, tautomers were taken into account (treated as conformers in the COSMOtherm calculation), as considering only a single tautomer may lead to substantial differences in predicted log $K_{hex/w}$. For sulfadiazine, we observed an exceptionally wide range of predicted log $K_{hex/w}$ across different tautomers, spanning from –3.5 to –13, potentially increasing uncertainties in the $K_{hex/w}$ calculation.

When UFZ-preselected LSER descriptors are unavailable, COSMOtherm appears to be the more suitable method for predicting log $K_{hex/w}$ compared to the UFZ-LSER database. This is evident from the substantially lower RMSE of 1.02 ($n = 64$) for the COSMOtherm prediction,

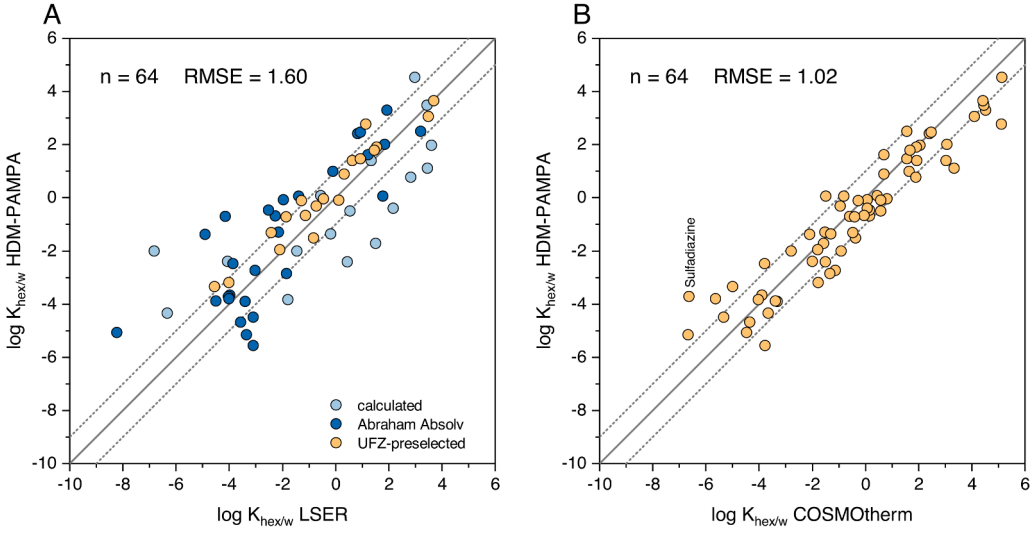

Fig. 2. Comparison of log $K_{hex/w}$ derived from HDM-PAMPA assays (see Table S1–5) with A) log $K_{hex/w}$ predicted by the UFZ-LSER database (see Table S1–7) and B) log $K_{hex/w}$ predicted by COSMOtherm (see Table S1–7). The gray solid line represents the line of identity, deviations of ±1 log unit are shown as gray dotted lines.

compared to the RMSE of 1.60 ($n = 64$) for the LSER prediction based on the highest-quality available descriptors (experimental or calculated). The discrepancy becomes even more pronounced when, instead of the best available LSER descriptors, only predicted LSER descriptors are used, increasing the RMSE further to 1.90 ($n = 64$), see Fig. S1–1. The same trend is observed when using literature-derived $K_{hex/w}$ instead of our own (see Fig. S1–2). However, the COSMOtherm approach is considerably more time- and computationally intensive.

3.3. Comparison of experimental and predicted log $P_{0,Caco\text{-}2/MDCK}$

3.3.1. Prediction of $P_{0,Caco\text{-}2/MDCK}$ based on experimental $K_{hex/w}$

The objective of generating a reliable $K_{hex/w}$ was to enable the prediction of $P_{0,Caco\text{-}2/MDCK}$ according to Eqs. (1) and (2). To validate this approach, we compared experimental $P_{0,Caco\text{-}2/MDCK}$ collected by Ebert et al. (2024) with predicted $P_{0,Caco\text{-}2/MDCK}$ based on HDM-PAMPA derived $K_{hex/w}$ (see Fig. 3A).

We observed a strong agreement between experimental and predicted $P_{0,Caco\text{-}2/MDCK}$ ($n = 29$, RMSE = 0.80), demonstrating that the prediction of $P_{0,Caco\text{-}2/MDCK}$ from HDM-PAMPA-derived $K_{hex/w}$ is accurate. Minor deviations may be attributed to uncertainties in the experimental $K_{hex/w}$ caused by sorption to plastics or evaporation as well as uncertainties in the experimental $P_{0,Caco\text{-}2/MDCK}$ caused by underestimating the influence of ABL and paracellular transport or recovery issues (Ebert et al., 2024). To put the error of 0.8 log units into perspective, a comparison with the performance of $P_{app,Caco\text{-}2/MDCK}$ predictions is not meaningful, since those typically span only about 2–3 orders of magnitude, whereas our $P_{0,Caco\text{-}2/MDCK}$ values cover approximately 7 orders of magnitude, and the two parameters often capture different underlying transport processes. A more appropriate comparison is therefore with other $P_{0,Caco\text{-}2/MDCK}$ predictions: the error is somewhat higher than the 0.48 log units we previously reported for BLM-based predictions (Dahley et al., 2024), although that smaller dataset (n = 14) is not directly comparable, as it was used to establish the correlation in Eq. (1), while here we used our dataset for external validation. The 0.8 log unit error is also close to the 0.68 reported by Avdeef (2012) for $P_{0,Caco\text{-}2/MDCK}$ predictions from *in combo*-PAMPA, but that correlation was trained on the Avdeef dataset (n = 426), and the dataset still contained permeabilities influenced by factors other than membrane permeation, such as ABL effects (Dahley et al., 2023; Ebert et al., 2024). Therefore, the reported errors are not perfectly comparable.

3.3.2. Prediction of $P_{0,Caco\text{-}2/MDCK}$ based on predicted $K_{hex/w}$

To assess the accuracy of $P_{0,Caco\text{-}2/MDCK}$ predictions based on the predicted $K_{hex/w}$, we compared experimental $P_{0,Caco\text{-}2/MDCK}$ with predicted $P_{0,Caco\text{-}2/MDCK}$ based on LSER-derived (see Fig. 3B) and COSMOtherm-derived $K_{hex/w}$ (see Fig. 3C).

A comparison of Figs. 3A and 3B reveals that when UFZ-preselected LSER descriptors are used, predictions based on predicted log $K_{hex/w}$ achieve a similarly strong agreement between experimental and predicted $P_{0,Caco\text{-}2/MDCK}$ as predictions based on experimental $K_{hex/w}$ from HDM-PAMPA ($n = 10$, RMSE = 0.79). The degree of agreement between experimental and predicted $P_{0,Caco\text{-}2/MDCK}$ decreases only slightly when Abraham Absolv instead of UFZ-preselected descriptors are used to predict $K_{hex/w}$ ($n = 14$, RMSE = 0.99). This was unexpected, as Fig. 2A shows that $K_{hex/w}$ predicted from Abraham Absolv descriptors can significantly deviate from those derived from HDM-PAMPA experiments. The fact that both resulting $P_{0,Caco\text{-}2/MDCK}$ align reasonably well with experimental $P_{0,Caco\text{-}2/MDCK}$, despite large differences in $K_{hex/w}$, can be attributed to the experimental $P_{0,Caco\text{-}2/MDCK}$ falling between the predicted $P_{0,Caco\text{-}2/MDCK}$. As expected, using calculated descriptors to predict $K_{hex/w}$ resulted in poor agreement between predicted and experimental $P_{0,Caco\text{-}2/MDCK}$ ($n = 5$, RMSE = 2.48).

As expected from Fig. 2B, good agreement between experimental $P_{0,Caco\text{-}2/MDCK}$ and predicted $P_{0,Caco\text{-}2/MDCK}$, based on COSMOtherm-derived $K_{hex/w}$, was observed ($n = 29$, RMSE = 1.20). However, two outliers were identified where experimental and predicted $P_{0,Caco\text{-}2/MDCK}$ differ by more than two orders of magnitude. As explained in Section 3.2.2, the $K_{hex/w}$ predicted by COSMOtherm for sulfadiazine is likely incorrect, due to the presence of tautomers with significantly differing $K_{hex/w}$. Both HDM-PAMPA and the UFZ-LSER database provide a $K_{hex/w}$ that leads to a better prediction of $P_{0,Caco\text{-}2/MDCK}$. The $K_{hex/w}$ predicted by COSMOtherm for etoposide might also be incorrect, though the uncertainty here is not due to tautomers but possibly to the size of the molecule. With a molecular weight of 588.56 g/mol, etoposide is the largest molecule in the dataset and uncertainty in calculated $K_{hex/w}$ increases with the size of the molecule (Ulrich et al., 2021). Predictions for compounds with a molecular weight above 500 g/mol are thus less reliable. Nevertheless, in contrast to sulfadiazine, the COSMOtherm-derived log $K_{hex/w}$ of −3.56 still aligns reasonably well with the HDM-PAMPA-derived log $K_{hex/w}$ of −4.35, which might indicate that for etoposide, the experimental $P_{0,Caco\text{-}2/MDCK}$ might also be inaccurate.

The comparison between predicted and experimental $P_{0,Caco\text{-}2/MDCK}$ clearly shows that the most accurate predictions are obtained when using experimental $K_{hex/w}$ from HDM-PAMPA (RMSE = 0.80). The use of predicted $K_{hex/w}$ as an alternative to experimental $K_{hex/w}$ is possible but associated with greater uncertainty, as reflected in a higher RMSE. Although the RMSE value for predictions based on COSMOtherm (RMSE = 1.20) is only slightly lower than that for predictions based on best

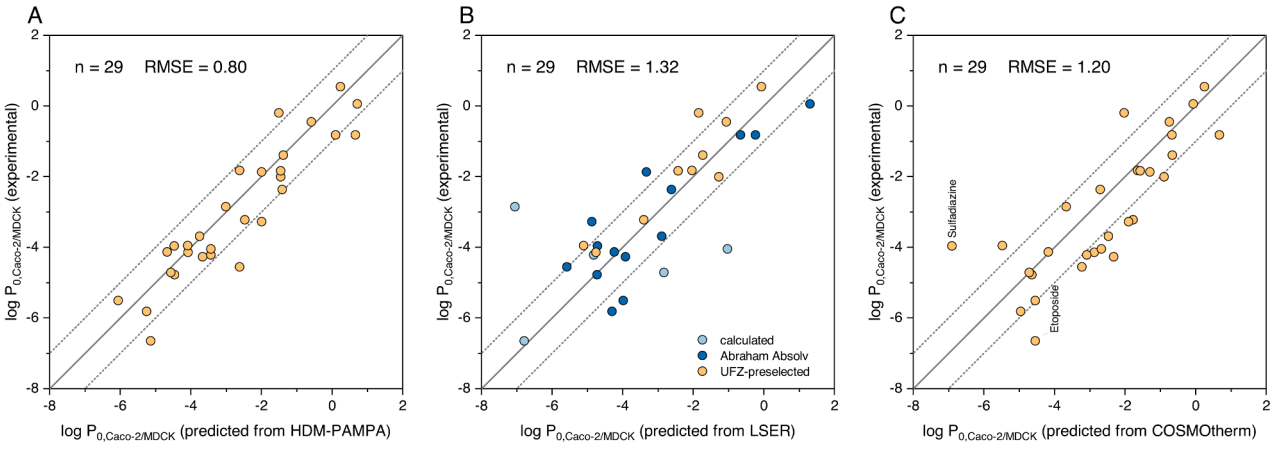

Fig. 3. Comparison of experimental log $P_{0,Caco\text{-}2/MDCK}$ with log $P_{0,Caco\text{-}2/MDCK}$ predicted according to Eqs. (1) and (2) using A) log $K_{hex/w}$ derived from HDM-PAMPA assays, B) log $K_{hex/w}$ predicted by the UFZ-LSER database and C) log $K_{hex/w}$ predicted by COSMOtherm. The gray solid line represents the line of identity, deviations of ±1 log unit are shown as gray dotted lines.

available LSER descriptors (RMSE = 1.32), it clearly outperforms predictions based solely on calculated UFZ-LSER descriptors (RMSE = 1.63, see Fig. S1–3). This is notable given that the LSER model is trained on 24 of the 29 compounds - making this comparison inherently biased in favor of the LSER approach. Although the UFZ-LSER database is generally less accurate than COSMOtherm for the $K_{hex/w}$ predictions, comparing the two methods can still provide valuable context. When both approaches yield similar results, confidence in the predicted value is increased. If the predictions diverge, COSMOtherm is still considered more reliable, but caution is warranted when interpreting the value. Notably, the two strong outliers - sulfadiazine and etoposide - with deviations exceeding 2 log units between experimental and predicted $P_{0,Caco\text{-}2/MDCK}$ values, also differed by >2.5 log units between the two computational methods.

4. Conclusion

HDM-PAMPA is a robust and reliable tool for experimentally determining log $K_{hex/w}$. This is evident from the strong agreement between log $K_{hex/w}$ obtained from HDM-PAMPA in this work and those obtained from conventional two-phase systems, BLM permeability assays and other HDM-PAMPA studies in the literature. However, for high quality results it is crucial to ensure that potential errors caused by sorption to plastic, evaporation, the formation of air bubbles between buffer and hexadecane layer or ABL limitations are carefully avoided during the experiment.

The log $K_{hex/w}$ from HDM-PAMPA can be successfully used to predict $P_{0,Caco\text{-}2/MDCK}$ according to Eq. (1). As an alternative to experimental determination in HDM-PAMPA, log $K_{hex/w}$ can be accurately predicted using COSMOtherm, although prediction uncertainties tend to increase with molecular size, particularly for compounds exceeding 500 g/mol. The prediction of log $K_{hex/w}$ by the UFZ-LSER database, however, is only reliable when UFZ-preselected descriptors are available.

Funding

This research did not receive any specific grant from funding agencies in the public, commercial, or not-for-profit sectors.

CRediT authorship contribution statement

Carolin Dahley: Writing – original draft, Visualization, Methodology, Investigation, Formal analysis. **Kai-Uwe Goss:** Writing – review & editing, Supervision, Conceptualization. **Andrea Ebert:** Writing – review & editing, Investigation, Formal analysis, Conceptualization.

Declaration of competing interest

The authors declare that they have no known competing financial interests or personal relationships that could have appeared to influence the work reported in this paper.

Supplementary materials

Supplementary material associated with this article can be found, in the online version, at doi:10.1016/j.ejps.2025.107280.

Data availability

Data will be made available on request.

References

ACD/Percepta, 2020. version 2020.1.2, Advanced Chemistry Development, Inc. (ACD/Labs), Toronto, ON, Canada. www.acdlabs.com.

Assmus, F., Ross, A., Fischer, H., Seelig, J., Seelig, A., 2017. 31P and 1H NMR studies of the Molecular organization of lipids in the parallel artificial membrane permeability assay. Mol Pharm 14 (1), 284–295. https://doi.org/10.1021/acs.molpharmaceut.6b00889.

Avdeef, A., 2012. Absorption and Drug development: Solubility, permeability, and Charge State, 2nd ed. John Wiley & Sons, Hoboken N.J.

Bahadur, N.P., Shiu, W.-Y., Boocock, D.G.B., Mackay, D., 1997. Temperature dependence of octanol−water partition coefficient for selected chlorobenzenes. J Chem Eng Data 42 (4), 685–688. https://doi.org/10.1021/je970020p.

Berthelot, M., Jungfleisch, E., 1872. Sur les lois qui président au partage d'un corps entre deux dissolvants (expériences). Ann Chim Phys 4 (26), 396–407.

Bittermann, K., Goss, K.-U., 2017. Predicting apparent passive permeability of Caco-2 and MDCK cell-monolayers: a mechanistic model. PloS one 12 (12), e0190319. https://doi.org/10.1371/journal.pone.0190319.

Bujard, A., Petit, C., Carrupt, P.-A., Rudaz, S., Schappler, J., 2017. HDM-PAMPA to predict gastrointestinal absorption, binding percentage, equilibrium and kinetics constants with human serum albumin and using 2 end-point measurements. Eur J Pharm Sci 97, 143–150. https://doi.org/10.1016/j.ejps.2016.11.001.

Bujard, A., Sol, M., Carrupt, P.-A., Martel, S., 2014. Predicting both passive intestinal absorption and the dissociation constant toward albumin using the PAMPA technique. Eur J Pharm Sci 63, 36–44. https://doi.org/10.1016/j.ejps.2014.06.025.

COSMOtherm, 2018. version C30, release 18, COSMOlogic GmbH & Co. KG, Leverkusen, Germany. www.cosmologic.de.

Dahley, C., Böckmann, T., Ebert, A., Goss, K.-U., 2024. Predicting the intrinsic membrane permeability of caco-2/MDCK cells by the solubility-diffusion model. Eur J Pharm Sci 195, 106720. https://doi.org/10.1016/j.ejps.2024.106720.

Dahley, C., Garessus, E.D.G., Ebert, A., Goss, K.-U., 2022. Impact of cholesterol and sphingomyelin on intrinsic membrane permeability. Biochim Biophys Acta Biomembr 1864 (9), 183953. https://doi.org/10.1016/j.bbamem.2022.183953.

Dahley, C., Goss, K.-U., Ebert, A., 2023. Revisiting the pKa-flux method for determining intrinsic membrane permeability. Eur J Pharm Sci 191, 106592. https://doi.org/10.1016/j.ejps.2023.106592.

Dearden, J.C., Bresnen, G.M., 1988. The measurement of partition coefficients. Quant Struct-Act Relat 7 (3), 133–144. https://doi.org/10.1002/qsar.19880070304.

Di, L., Artursson, P., Avdeef, A., Benet, L.Z., Houston, J.B., Kansy, M., Kerns, E.H., Lennernäs, H., Smith, D.A., Sugano, K., 2020. The critical role of passive permeability in designing successful drugs. ChemMedChem 15 (20), 1862–1874. https://doi.org/10.1002/cmdc.202000419.

Ebert, A., Dahley, C., Goss, K.-U., 2024. Pitfalls in evaluating permeability experiments with Caco-2/MDCK cell monolayers. Eur J Pharm Sci 194, 106699. https://doi.org/10.1016/j.ejps.2024.106699.

Eckert, F., Klamt, A., 2002. Fast solvent screening via quantum chemistry: COSMO-RS approach. AIChE J 48 (2), 369–385. https://doi.org/10.1002/aic.690480220.

EAS-E Suite, 2025. Ver.0.98 - BETA, release April. www.eas-e-suite.com. Accessed [01.07.2025]. Developed by ARC Arnot Research and Consulting Inc., Toronto, ON, Canada.

Endo, S., Goss, K.-U., 2014. Applications of polyparameter linear free energy relationships in environmental chemistry. Environ Sci Technol 48 (21), 12477–12491. https://doi.org/10.1021/es503369t.

Fagerholm, U., 2008. The role of permeability in drug ADME/PK, interactions and toxicity–presentation of a permeability-based classification system (PCS) for prediction of ADME/PK in humans. Pharm Res 25 (3), 625–638. https://doi.org/10.1007/s11095-007-9397-y.

Finkelstein, A., 1976. Water and nonelectrolyte permeability of lipid bilayer membranes. J Gen Physiol 68 (2), 127–135. https://doi.org/10.1085/jgp.68.2.127.

Hubatsch, I., Ragnarsson, E.G.E., Artursson, P., 2007. Determination of drug permeability and prediction of drug absorption in Caco-2 monolayers. Nat Protoc 2 (9), 2111–2119. https://doi.org/10.1038/nprot.2007.303.

Klamt, A., 1995. Conductor-like screening model for real solvents: a new approach to the quantitative calculation of solvation phenomena. J Phys Chem 99 (7), 2224–2235. https://doi.org/10.1021/j100007a062.

Klamt, A., Jonas, V., Bürger, T., Lohrenz, J.C.W., 1998. Refinement and parametrization of COSMO-RS. J Phys Chem A 102 (26), 5074–5085. https://doi.org/10.1021/jp980017s.

Lomize, A.L., Pogozheva, I.D., 2019. Physics-based method for modeling passive membrane permeability and translocation pathways of bioactive molecules. J Chem Inf Model 59 (7), 3198–3213. https://doi.org/10.1021/acs.jcim.9b00224.

Nagahara, N., Tavelin, S., Artursson, P., 2004. Contribution of the paracellular route to the pH-dependent epithelial permeability to cationic drugs. J Pharm Sci 93 (12), 2972–2984. https://doi.org/10.1002/jps.20206.

Nielsen, P.E., Avdeef, A., 2004. PAMPA–a drug absorption in vitro model 8. Apparent filter porosity and the unstirred water layer. Eur J Pharm Sci 22 (1), 33–41. https://doi.org/10.1016/j.ejps.2004.02.003.

Petit, C., Bujard, A., Skalicka-Woźniak, K., Cretton, S., Houriet, J., Christen, P., Carrupt, P.-A., Wolfender, J.-L., 2016. Prediction of the passive intestinal absorption of medicinal plant extract constituents with the parallel artificial membrane permeability assay (PAMPA). Planta Med 82 (5), 424–431. https://doi.org/10.1055/s-0042-101247.

Rolando, B., Lazzarato, L., Di Stilo, A., Fruttero, R., Carrupt, P.-A., Martel, S., Gasco, A., 2010. Physicochemical profile and in vitro permeation behavior of a new class of non-steroidal anti-inflammatory drug candidates. Eur J Pharm Sci 40 (3), 217–221. https://doi.org/10.1016/j.ejps.2010.03.015.

Tsinman, O., Tsinman, K., Sun, N., Avdeef, A., 2011. Physicochemical selectivity of the BBB microenvironment governing passive diffusion–matching with a porcine brain lipid extract artificial membrane permeability model. Pharm Res 28 (2), 337–363. https://doi.org/10.1007/s11095-010-0280-x.

UFZ-LSER, 2025. database v4.0 [Internet], Leipzig, Germany, Helmholtz Centre for Environmental Research-UFZ [accessed on 01.07.2025]. Available from. https://www.ufz.de/lserd.

Ulrich, N., Goss, K.-U., Ebert, A., 2021. Exploring the octanol-water partition coefficient dataset using deep learning techniques and data augmentation. Commun Chem 4 (1), 90. https://doi.org/10.1038/s42004-021-00528-9.

Von Richter, O., Glavinas, H., Krajcsi, P., Liehner, S., Siewert, B., Zech, K., 2009. A novel screening strategy to identify ABCB1 substrates and inhibitors. Naunyn Schmiedebergs Arch Pharmacol 379 (1), 11–26. https://doi.org/10.1007/s00210-008-0345-0.

Walter, A., Gutknecht, J., 1984. Monocarboxylic acid permeation through lipid bilayer membranes. J Membr Biol 77 (3), 255–264. https://doi.org/10.1007/BF01870573.

Walter, A., Gutknecht, J., 1986. Permeability of small nonelectrolytes through lipid bilayer membranes. J Membr Biol 90 (3), 207–217. https://doi.org/10.1007/BF01870127.

Wohnsland, F., Faller, B., 2001. High-throughput permeability pH profile and high-throughput alkane/water log P with artificial membranes. J Med Chem 44 (6), 923–930. https://doi.org/10.1021/jm001020e.

Yazdanian, M., Glynn, S.L., Wright, J.L., Hawi, A., 1998. Correlating partitioning and caco-2 cell permeability of structurally diverse small molecular weight compounds. Pharm Res 15 (9), 1490–1494. https://doi.org/10.1023/a:1011930411574.